Enhanced stability and ultrahigh proton conductivity of hydrogen-bonded organic framework

Qianqian Yang[#], Xinyu Li[#], Changsong Xie, Zhen Wang, Zhihui Kong, Jianjian Yang, Zixi Kang, Rongming Wang,* Daofeng Sun

School of Materials Science and Engineering, College of Chemistry and Chemical Engineering, China University of Petroleum (East China), Qingdao Shandong 266580, China

[#] these authors contributed equally to this work

E-mail: rmwang@upc.edu.cn

Materials. 4,4'-diamino-2,2'-stilbenedisulfonic acid (DSD acid) (95%, Sahn Chemical Technology (Shanghai) Co., Ltd.), 1,3,5-triformyl phloroglucinol (Tp) (98%, Zhengzhou Ruke Biotechnology Co., Ltd.), p-toluenesulfonic acid monohydrate (PTSA) (98%, Sahn Chemical Technology (Shanghai) Co., Ltd.), sodium hydroxide (NaOH) (AR, Sinopharm Chemical Reagent Co., Ltd.), ammonia solution (NH_4OH) (AR, Sinopharm Chemical Reagent Co., Ltd.), glacial acetic acid (HAc) (AR, Sinopharm Chemical Reagent Co., Ltd.), N,N-dimethyformamide (DMF) (AR, Sinopharm Chemical Reagent Co., Ltd.), 1,4-dioxane (AR Sinopharm Chemical Reagent Co., Ltd.), tetrahydrofuran (THF) (AR, Tianjin Fuyu Fine Chemical Co., Ltd), acetonitrile (AR, Tianjin Fuyu Fine Chemical Co., Ltd), deionized water. All chemicals were purchased and directly used without further purification.

Growth of HDSD-1 single crystals: 10 mg of DSD acid, 10 mL of deionized water and 10 μL of NaOH (6 mol/L) was placed in a 20 mL vial, and then sealed and sonicated until completely dissolved. After transferring half of the solution to the petri dish with a diameter of 8 centimeter, place a vial containing 1 mLHAc (6 mol/L) in it, then seal the petri dish for 24 hours to obtain single crystal of HDSD-1. Anal. (%) calcd for HDSD-1 ($C_{14}H_{14}O_6N_2S_2$): C, 45.40; H, 3.81; N, 7.56. Found: C, 44.76; H,3.86; N, 7.41.

Synthesis of HDSD-1@TP: After 33.3 mg (0.09 mmol) HDSD-1 and 100 mg (0.58 mmol) of PTSA were mixed and ground in a mortar for 10 minutes, 12.6 mg (0.06 mmol) of Tp was added and ground mixture for 10 minutes. The mixture was transferred to a 10 mL vial using 2 mL of deionized water, then sealed it up and heated in an oven at 90 ^oC for 3 days. Subsequently, the product were filtered and

washed with the mixed solution of DMF and water (1:1), 1,4-dioxane, and THF. The obtained solid was further immersed in acetonitrile to remove the possible impurity for three times. Finally, the product was dried in vacuum at 120 °C for 12 hours to get HDSD-1@TP. Anal. (%) calcd for HDSD-1@0.1TP·H_2O ($C_{14.9}H_{16}O_{7.3}N_2S_2$): C, 44.29; H, 4.02; N, 7.03. Found: C, 44.29; H,3.99; N, 6.93.

Preparation of the HDSD-1@TP-NH_3: 5 mg HDSD-1@TP was exposed to vapors of 2 mL of $NH_3·H_2O$ (6 mol/L) at room temperature for 2 hours, giving HDSD-1@TP-NH_3. Anal. (%) calcd for HDSD-1@0.1TP·2NH_3·0.8H_2O ($C_{14.9}H_{21.6}O_{7.1}N_4S_2$): C, 41.59; H, 4.93; N, 12.81. Found: C, 41.19; H,5.01; N, 12.90.

Preparation of 5% HDSD-1@Tp-NH_3/Nafion: HDSD-1@TP-NH_3 (60 mg) was added to Nafion solution (20wt%, 6 g), and then the mixture was stirred at room temperature for 6 h to obtain a uniform solution. The resulting mixture was poured onto a slide and dried at room temperature for 24 hours to obtain 5% HDSD-1@Tp-NH_3/Nafion membrane.

Material characterization: Powder X-ray diffraction study of samples were done in a Rigaku Ultima IV X-Ray diffractometer using Cu-K α (λ =0.15406 nm) radiation. Diffraction patterns in the wide-angle region (3°−50°) were recorded at a rate of (2θ) = 5° min^{-1}. Thermal gravimetric analysis (TGA) was proceeded on a Mettler Toledo TGA instrument in the range of 40-900 °C with a heating rate of 10 °C min^{-1} under N_2 atmosphere (100 mL min^{-1}). Infrared (FTIR) spectra were obtained on a Nicolet 330 FTIR spectrometer. Scanning electron microscope (SEM) was collected by a Philips XL30 FEG SEM. N_2 and CO_2 adsorption and desorption tests were performed on a Micromeritics ASAP 2020 surface area analyzer. The pore size distribution was estimated from the 77K N_2 isotherms using a Slit Pore Geometry (original H-K) model fit.

Proton conductivity measurement. The resultant powder was pressed into a sample of 3 mm diameter and a thickness of 0.41 mm. Next, samples were fixed with two gold lines and coated with silver colloid on both sides, then dried it naturally. Impedance analysis was performed with a 1260A Impedance/Gain-Phase Analyzer from 10 MHz to 0.1 Hz with an input voltage 200 mV in a constant temperature and humidity, which were controlled by using a BPS-50CL humidity control chamber.

Each sample was pressed at least three tablets, and repeated cyclic tests were performed on each tablet. Typically, the impedance at each temperature were measured after equilibration for a period of 1 h. The resistance values were obtained by fitting the impedance profile using zview software. Proton conductivity (σ, S cm^{-1}) of each sample was obtained by the following equation:

$$\sigma = \frac{l}{RS}$$

where l and S are the length (cm) and area (cm^2) of the plate, respectively, and R is the intrinsic resistance value (Ω) of the material fitted by the equivalent circuit of the first semicircle using zview software. The activation energy (E_a) of the material is estimated according to the following Arrhenius equation:

$$\sigma T = \sigma_0 \, exp(-\frac{E_a}{k_B T})$$

Where σ_0 is the pre-exponential factor, T is the temperature, and k_B is the Boltzmann constant.

Fabrication of the Fuel Cell Assembly. PEMFCs are manufactured by sandwiching 5% HDSD-1@Tp-NH_3/Nafion or recast Nafion membranes between two gas diffusion electrodes. Catalyst inks were prepared by dispersing Pt/C black nanoparticles (Johnson Matthey, 70% Pt) into deionized water, isopropyl alcohol, and 20 wt % Nafion aqueous solution (Dupont). The catalyst ink is then sprayed onto carbon paper (Toray, YSLS30T) to form the cathode and anode respectively. The catalyst load was 0.5 mg·cm^{-2}. The electrode assemblies were prepared by mechanical hot extrusion for 30 s. PEMFC polarization curves and the long term durability test of PEMFCs at 0.5 V were obtained at 80 ^oC, 98% RH using a fuel cell test system (Dilian Yuke, YK-A10) with an effective area of 5 × 5 cm^2 under H_2 flow rate of 1.5 SLPM, air flow rate of 2.5 SLPM, and back pressure of 1 bar.

Table S1. Crystallographic and Refinement Parameters for HDSD-1

Crystal data	**HDSD-1**
System	monoclinic
Space group	$P2_1/c$
MF	$C_{14}H_{14}N_2O_6S_2$
FW	370.39
a/Å	10.8632(15)
b/Å	8.7447(10)
c/Å	7.5251(11)
α/°	90
β/°	90.0001(1)
γ/°	90
Volume/ Å^3	714.85(17)
Z	2
Density/g·cm^3	1.721
μ/mm^{-1}	3.743
F(000)	384.0
R_1[a] I>2θ	0.0648
R_{w2}[b] I>2θ	0.1745
R_1[a]	0.0743
R_{w2}[b]	0.1899

[a] $R_1 = \Sigma|Fo-|Fc||/\Sigma|Fo|$, [b] $Rw_2 = [\Sigma w(Fo^2-Fc^2)^2/\Sigma w(Fo^2)^2]^{1/2}$.

Table S2. The lengths (Å) angles (°) of hydrogen bonds in HDSD-1.

Bonds	Lengths/Å	Angle/°
N1-H1A…O3	2.31	142
N1-H1B…O2	1.84	176
N1-H1C…O1	1.93	157

Table S3. The humidity-dependent proton conductivity of HDSD-1, HDSD-1@TP and HDSD-1@TP-NH_3 at 80°C.

	HDSD-1 (S cm^{-1})	HDSD-1@TP (S cm^{-1})	HDSD-1@TP-NH_3 (S cm^{-1})
50%	1.3×10^{-6}	6.2×10^{-6}	5.9×10^{-4}
60%	5.8×10^{-6}	2.0×10^{-5}	1.0×10^{-3}
70%	3.6×10^{-5}	6.3×10^{-5}	2.0×10^{-3}
80%	1.7×10^{-4}	1.8×10^{-4}	5.2×10^{-3}
90%	1.3×10^{-3}	6.4×10^{-4}	4.2×10^{-2}
98%	7.5×10^{-3}	1.8×10^{-3}	3.8×10^{-1}

Table S4. Proton conductivities of reported MOF and COF materials.

Composition	Conditions	Conductivity (S cm^{-1})	References
SCOF	80 °C, pure water	5.4×10^{-1}	1
HDSD-1@TP-NH_3	80 °C, 98% RH	3.8×10^{-1}	This work
SPEEK/H_3PO_4@CTFp	80 °C, 100% RH	3.13×10^{-1}	2
SP-ZIF-L@GO-5	70 °C, 100% RH	2.65×10^{-1}	3
DHZIF-8/RN-3	80 °C, 95% RH	2.55×10^{-1}	4
IL-COF-SO_3H@SNF-35	90 °C, 100% RH	2.24×10^{-1}	5
Nafion/Z-COF-10	80 °C, 100% RH	2.2×10^{-1}	6
Cr-MIL-88B-PSA	100 °C, 85% RH	1.58×10^{-1}	7
IL-COF-SO_3H@SNF-15	90 °C, 100% RH	1.56×10^{-1}	5
Co-tri	80 °C, 98% RH	1.494×10^{-1}	8
10% ZUT-COF-SO_3H@Nafion	80 °C, 80% RH	1.34×10^{-1}	9
BUT-8(Cr)A	80 °C, 100% RH	1.27×10^{-1}	10
PCMOF2½ (Tz)	85 °C, 90% RH	1.17×10^{-1}	11
H_3PO_4@NKCOF-1	80 °C, 98% RH	1.13×10^{-1}	12
CS/A + B	30 °C, 98% RH	5.2×10^{-2}	13
H_3PO_4@NKCOF-2	80 °C, 98% RH	4.28×10^{-2}	12
$(NH_4)_2(adp)[Zn_2(ox)_3]\cdot nH_2O$	25 °C, 95% RH	8.0×10^{-3}	14
HDSD-1	80 °C, 98% RH	7.5×10^{-3}	This work
$[Pt_2(MPC)_4Cl_2Co(DMA)(HDMA)\cdot guest$	60 °C, 95% RH	7.1×10^{-3}	15
HDSD-1@TP	80 °C, 98% RH	1.8×10^{-3}	This work
ZZU-1	100 °C, 98% RH	8.9×10^{-4}	16
$[Gd(H_4NMP)(H_2O)_2]Cl\cdot 2H_2O$	80 °C, 95% RH	3.0×10^{-4}	7

ICG@HSB-W5	55 °C, 95% RH	2.18×10^{-4}	17
HKUST-1	55 °C, 98% RH	1.35×10^{-4}	18
$[CoCa(notpH_2)(H_2O)_2]ClO_4 \cdot 4H_2O$	25 °C, 95% RH	1.55×10^{-5}	19
$Zn_3(L7)(H_2O)_2 \cdot 2H_2O$ (PCMOF-3)	25 °C, 98% RH	3.5×10^{-5}	20

Table S5. The temperature-dependent proton conductivity of HDSD-1, HDSD-1@TP and HDSD-1@TP-NH_3 under 98% RH.

	HDSD-1 ($S\ cm^{-1}$)	HDSD-1@TP ($S\ cm^{-1}$)	HDSD-1@TP-NH_3 ($S\ cm^{-1}$)
40°C	1.3×10^{-3}	3.1×10^{-4}	7.4×10^{-2}
50°C	1.8×10^{-3}	5.0×10^{-4}	1.0×10^{-1}
60°C	3.0×10^{-3}	8.3×10^{-4}	1.5×10^{-1}
70°C	4.5×10^{-3}	1.3×10^{-3}	2.4×10^{-1}
80°C	7.5×10^{-3}	1.8×10^{-3}	3.8×10^{-1}

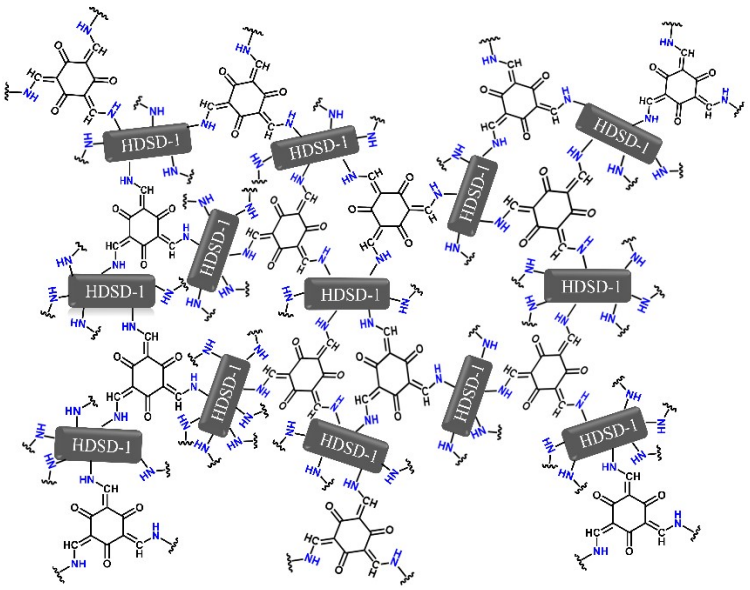

Scheme S1. The structure diagram of HDSD-1@Tp.

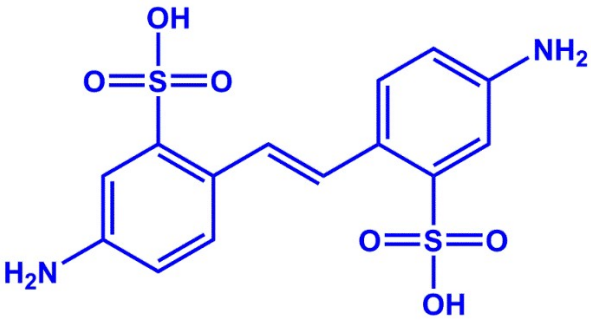

Fig. S1 DSD acid molecular structure.

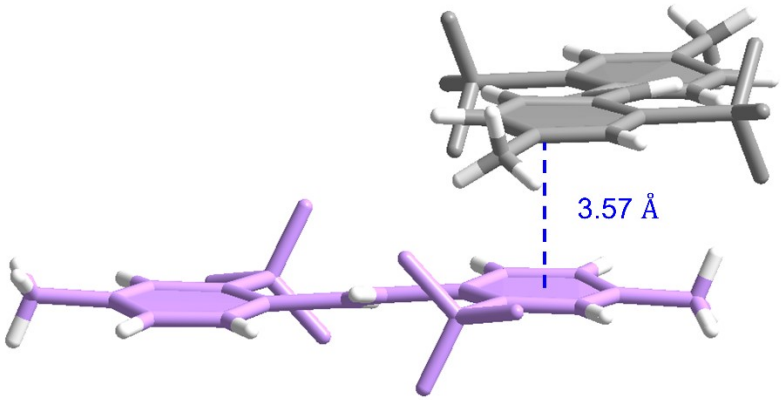

Fig. S2 The π-π stacking interactions in HDSD-1.

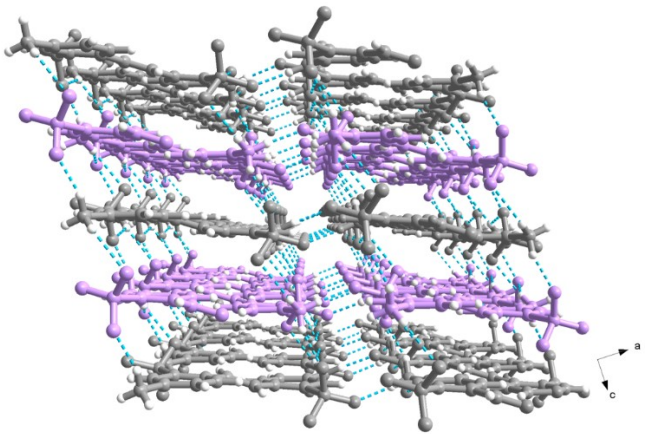

Fig. S3 Crystal structure of HDSD-1 viewed along b axis.

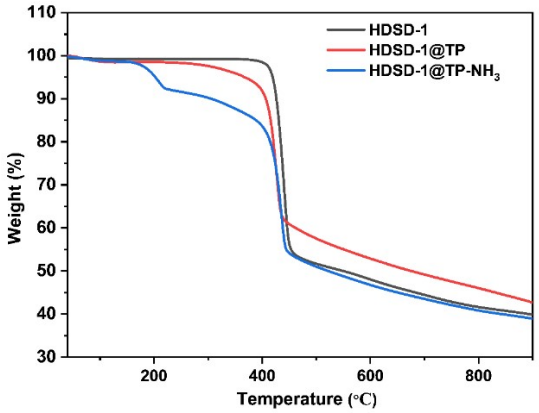

Fig. S4 TGA curves of HDSD-1, HDSD-1@Tp and HDSD-1@Tp-NH_3 in N_2 atmosphere.

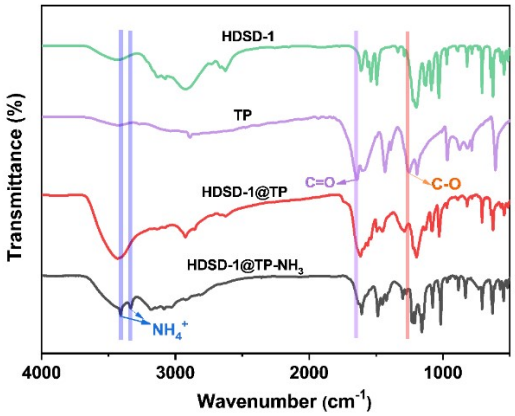

Fig. S5 FT-IR spectra of as-synthesized HDSD-1, TP, HDSD-1@Tp and HDSD-1@Tp-NH_3.

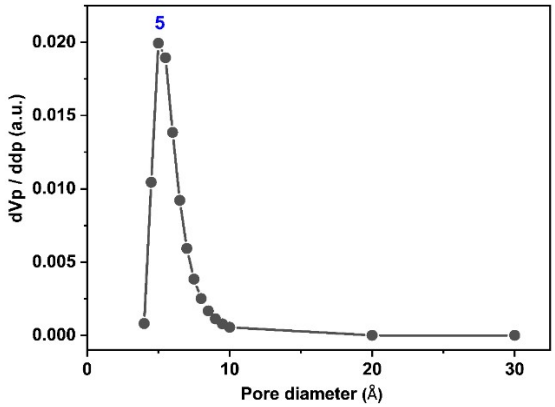

Fig. S6 Pore size distribution of HDSD-1@Tp.

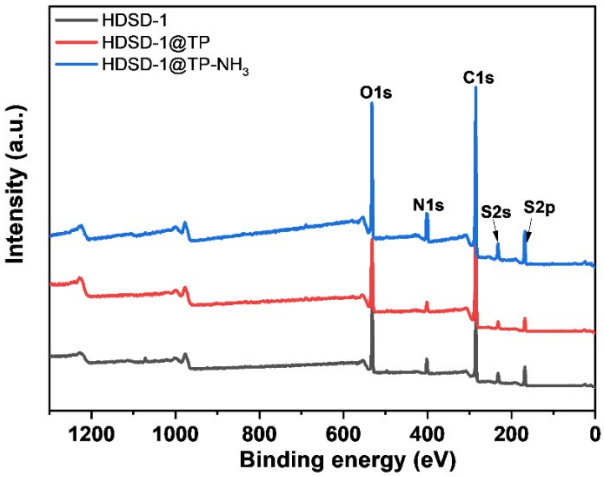

Fig. S7 The XPS spectra of HDSD-1, HDSD-1@Tp and HDSD-1@Tp-NH_3.

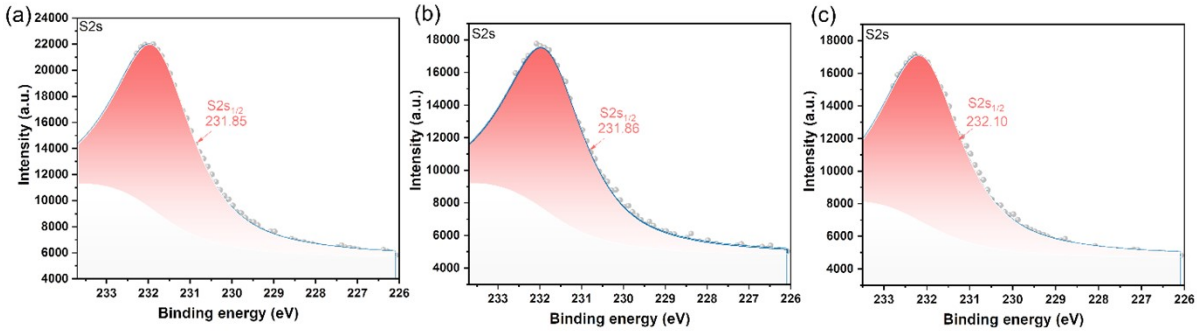

Fig. S8 The high-resolution XPS spectra of S2s for HDSD-1(a), HDSD-1@Tp (b) and HDSD-1@Tp-NH_3(c).

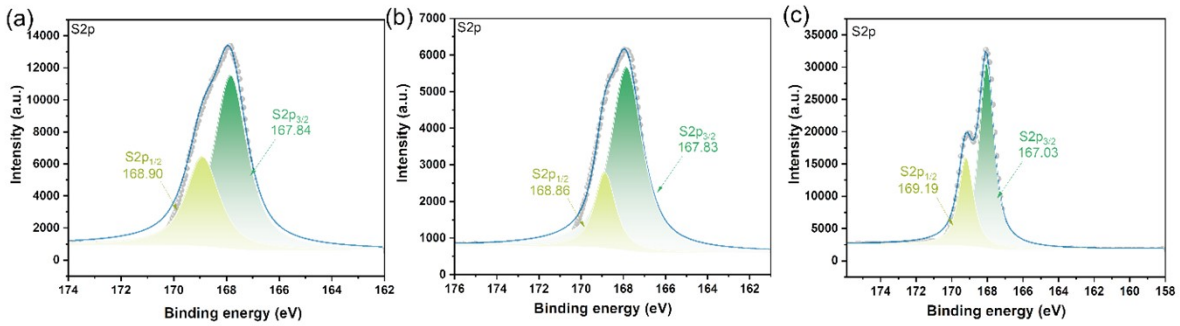

Fig. S9 The high-resolution XPS spectra of S2p for HDSD-1(a), HDSD-1@Tp (b) and HDSD-1@Tp-NH_3(c).

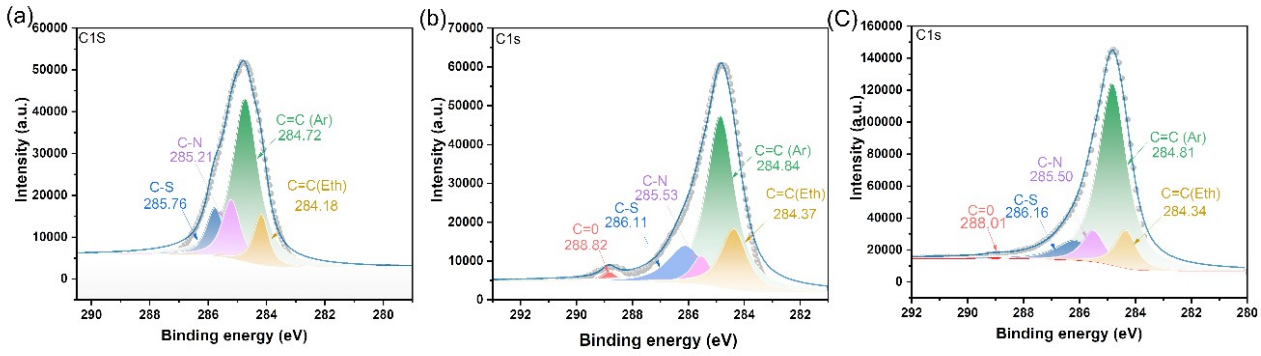

Fig. S10 The high-resolution XPS spectra of C1s for HDSD-1(a), HDSD-1@Tp(b) and HDSD-1@Tp-NH_3(c).

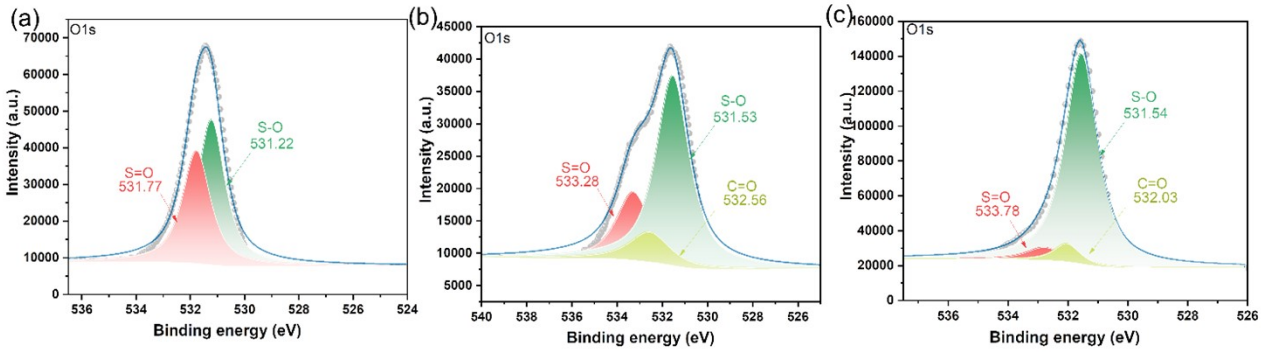

Fig. S11 The high-resolution XPS spectra of O1s for HDSD-1(a), HDSD-1@Tp (b) and HDSD-1@Tp-NH_3(c).

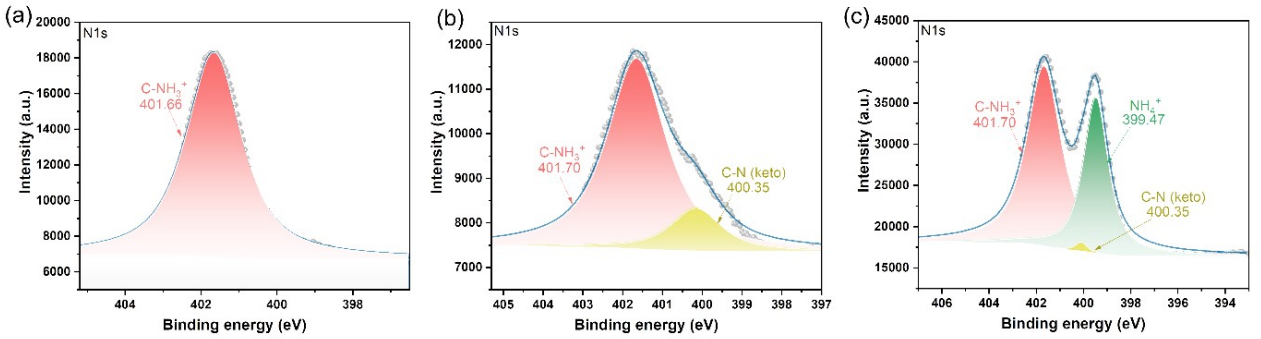

Fig. S12 The high-resolution XPS spectra of N1s for HDSD-1(a), HDSD-1@Tp (b) and HDSD-1@Tp-NH_3(c).

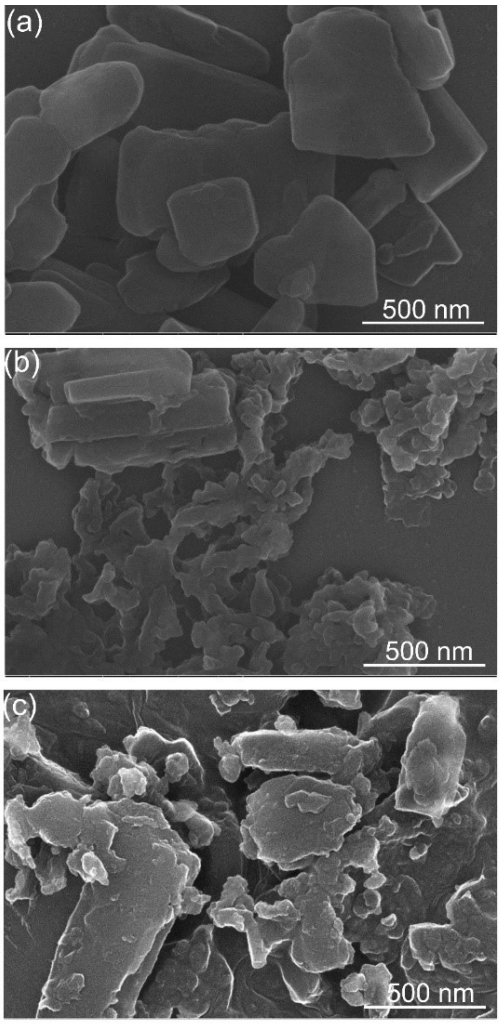

Fig. S13 The SEM images of HDSD-1 (a), HDSD-1@Tp (b) and HDSD-1@Tp-NH_3 (c).

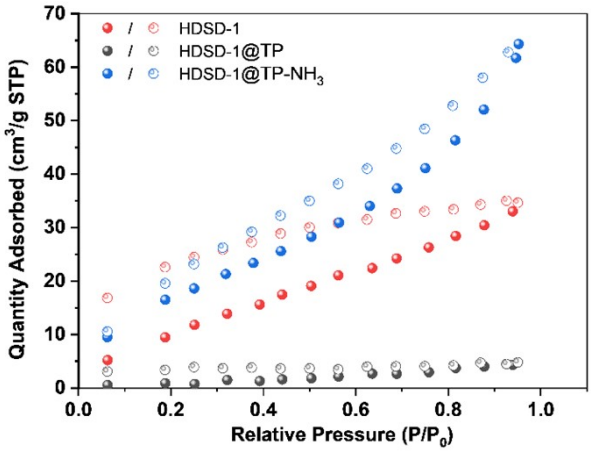

Fig. S14 Water adsorption (filled symbols) and desorption (empty symbols) isotherms of HDSD-1, HDSD-1@TP and HDSD-1@TP-NH_3

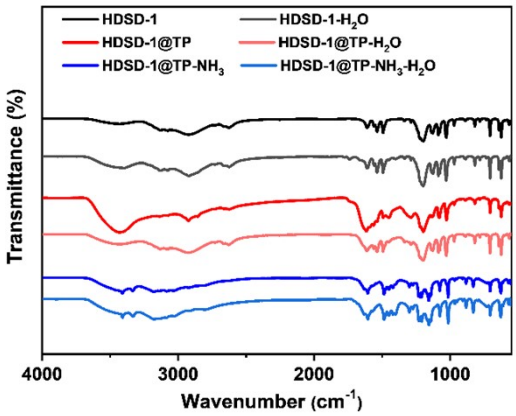

Fig. S15 FT-IR spectra of as-synthesized HDSD-1, HDSD-1-H_2O, HDSD-1@Tp, HDSD-1@Tp-H_2O, HDSD-1@Tp-NH_3 and HDSD-1@Tp-NH_3-H_2O.

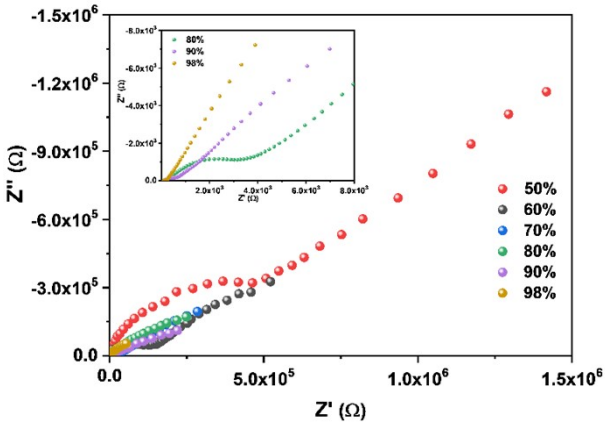

Fig. S16 Nyquist plot of HDSD-1 under different humidities at 80°C.

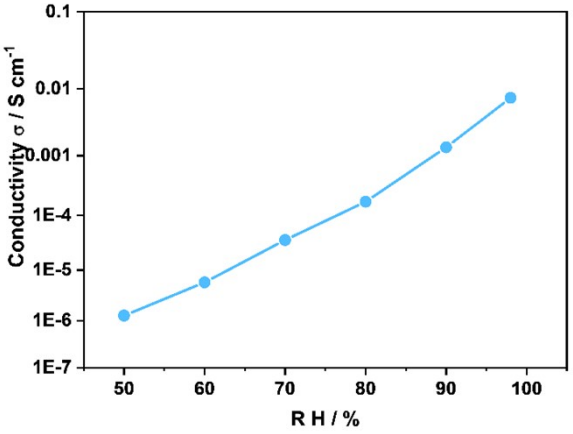

Fig. S17 Proton conductivities of HDSD-1 under different humidities at 80°C.

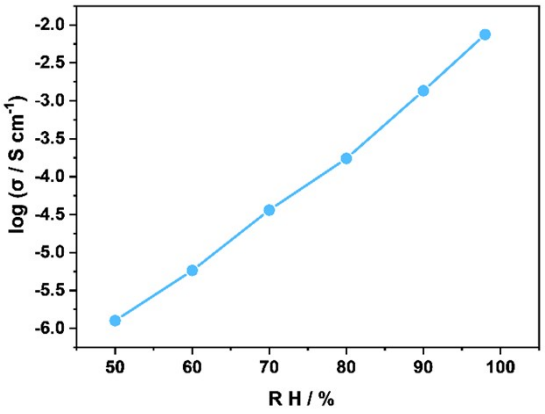

Fig. S18 Log-scaled proton conductivities of HDSD-1 under different humidities at 80°C.

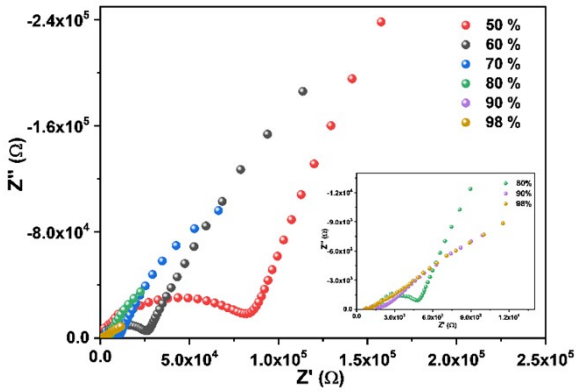

Fig. S19 Nyquist plot of HDSD-1@Tp under different humidities at 80°C.

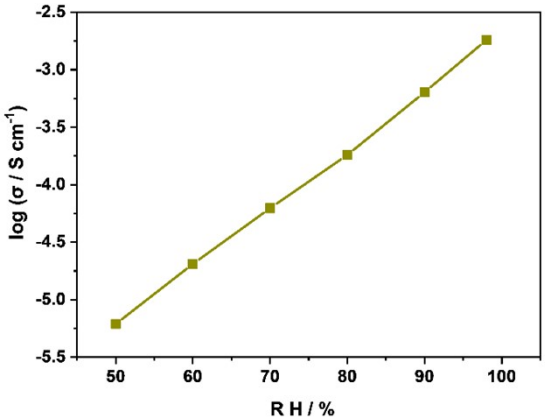

Fig. S20 Log-scaled proton conductivities of HDSD-1@Tp under different humidities at 80°C.

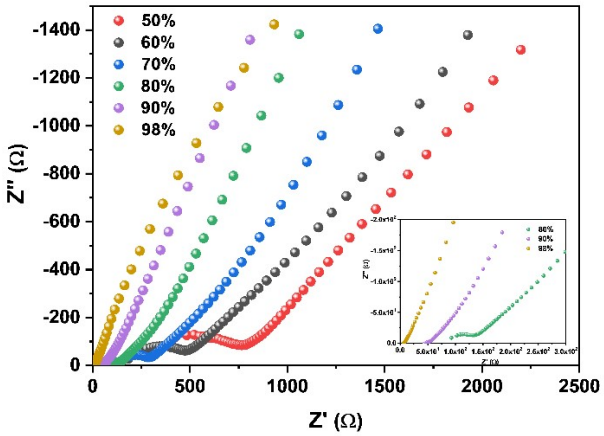

Fig. S21 Nyquist plot of HDSD-1@Tp-NH_3 under different humidities at 80°C.

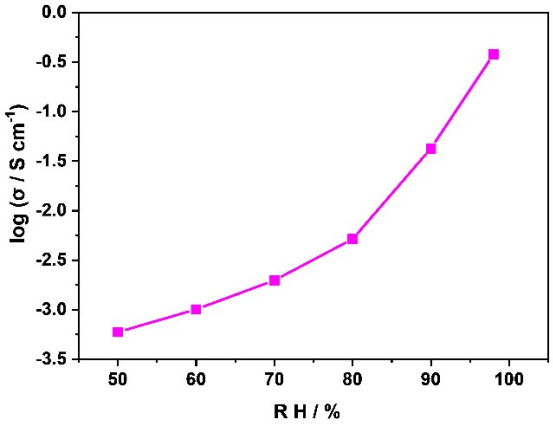

Fig. S22 Log-scaled proton conductivities of HDSD-1@Tp-NH_3 under different humidities at 80°C.

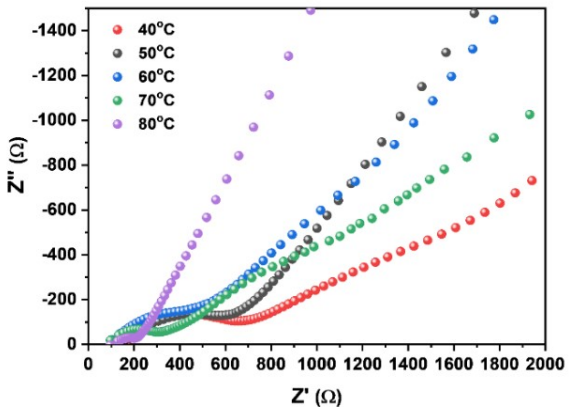

Fig. S23 Nyquist plot of HDSD-1 at different temperatures under 98% RH.

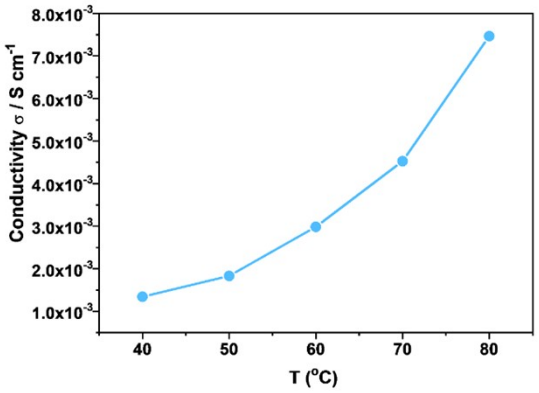

Fig. S24 Proton conductivities of HDSD-1 at different temperatures under 98% RH.

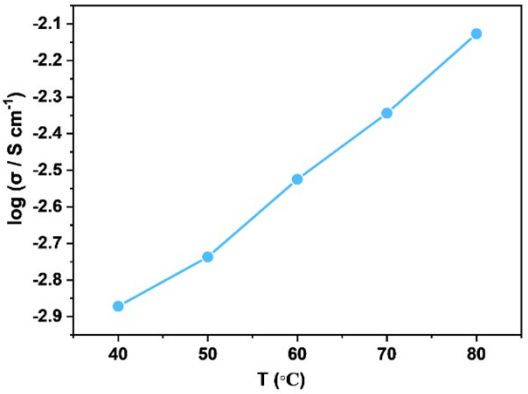

Fig. S25 Log-scaled proton conductivities of HDSD-1 at different temperatures under 98% RH.

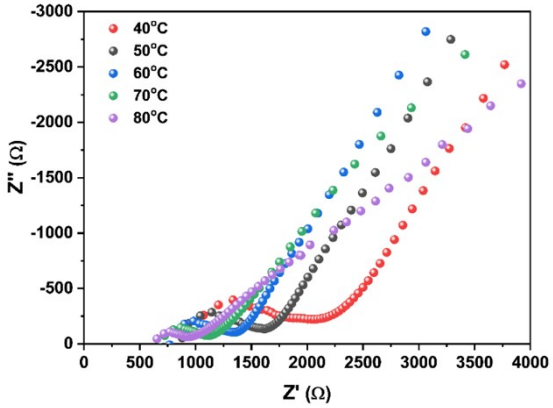

Fig. S26 Nyquist plot of HDSD-1@Tp at different temperatures under 98% RH.

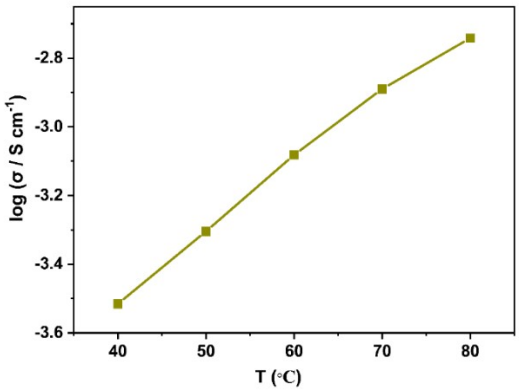

Fig. S27 Log-scaled proton conductivities of HDSD-1@Tp at different temperatures under 98% RH.

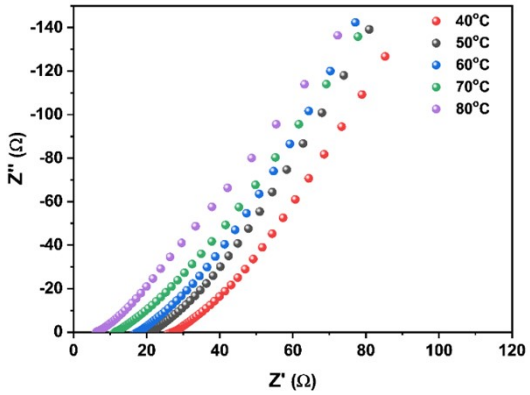

Fig. S28 Nyquist plot of HDSD-1@Tp-NH_3 at different temperatures under 98% RH.

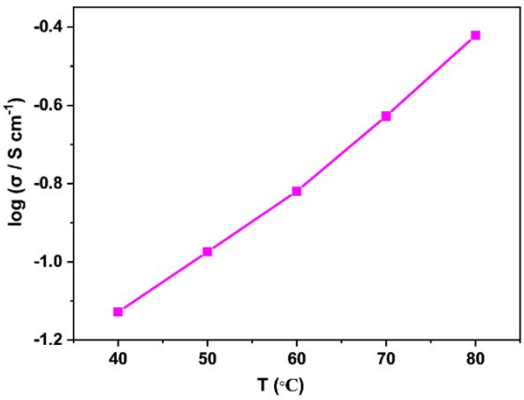

Fig. S29 Log-scaled proton conductivities of HDSD-1@Tp-NH_3 at different temperatures under 98% RH.

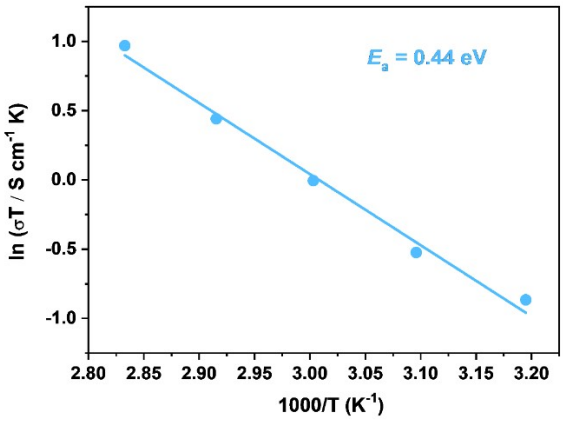

Fig. S30 Arrhenius plots of HDSD-1 under different temperature.

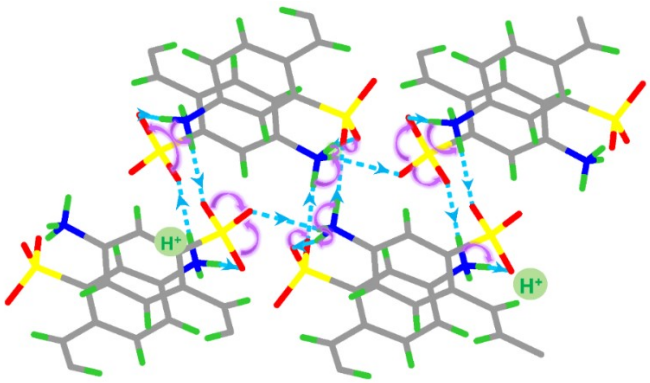

Fig. S31 The rotation diagram of NH_3^+ and SO_3^- in proton conduction for HDSD-1.

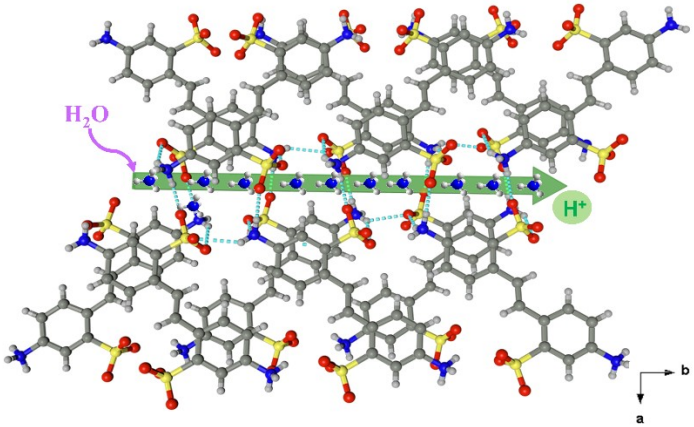

Fig. S32 The proton conduction pathways in HDSD-1@Tp-NH_3.

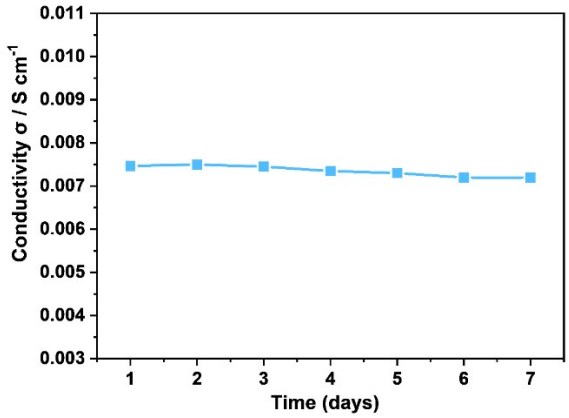

Fig. S33 Stability tests of HDSD-1 at 80°C under 98% RH.

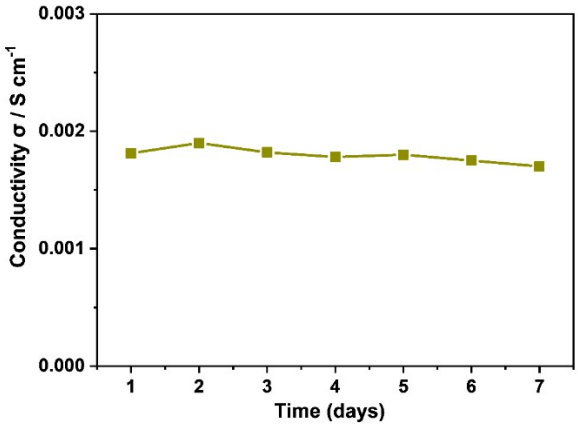

Fig. S34 Stability tests of HDSD-1@Tp at 80°C under 98% RH.

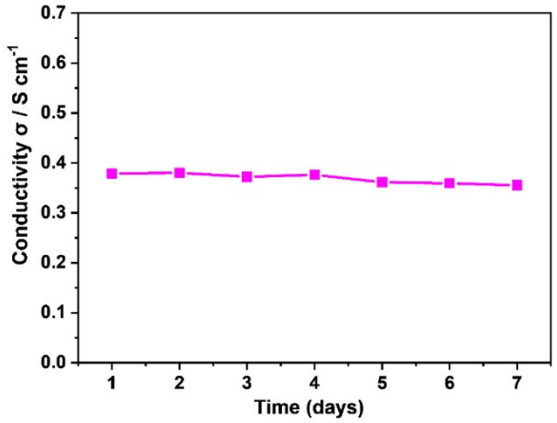

Fig. S35 Stability tests of HDSD-1@Tp-NH_3 at 80°C under 98% RH.

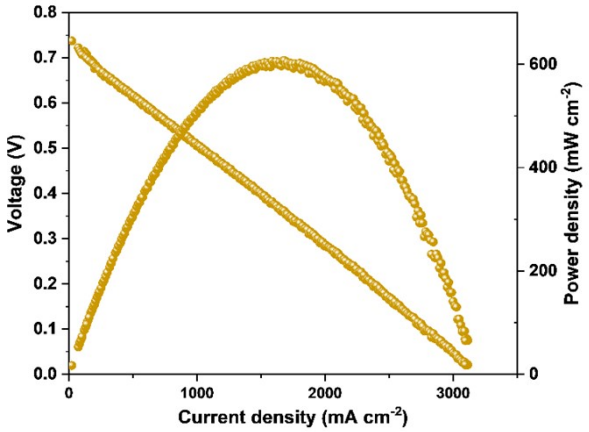

Fig. S36 Power density and current density of PEMFC for casting Nafion membrane.

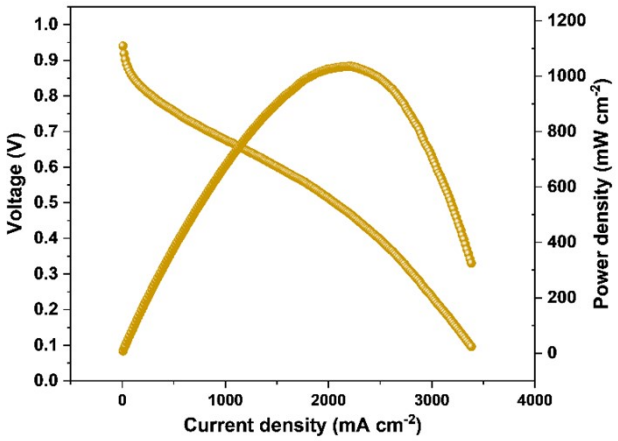

Fig. S37 Power density and current density of PEMFC for 5% HDSD-1@Tp-NH_3/Nafion composite membrane.

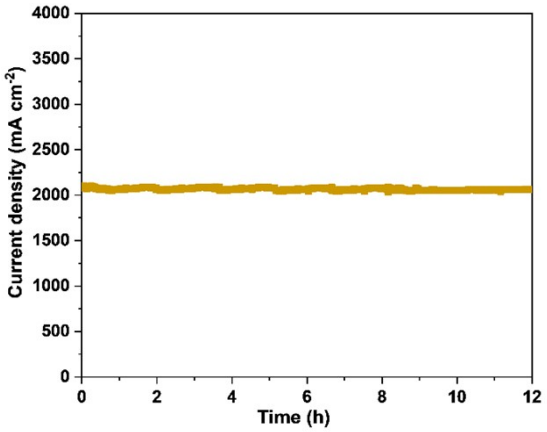

Fig. S38 Long term durability test of a single cell with 5% HDSD-1@Tp-NH_3/Nafion composite membrane at 0.5 V under 80 ^oC and 98% RH for 12 h.

References

1. L. Liu, L. Yin, D. Cheng, S. Zhao, H. Y. Zang, N. Zhang and G. Zhu, *Angew. Chem. Int. Ed. Engl.*, 2021, **60**, 14875-14880.
2. X. Sun, J.-H. Song, H.-q. Ren, X.-y. Liu, X.-w. Qu, Y. Feng, Z.-Q. Jiang and H.-l. Ding, *Electrochim. Acta*, 2020, **331**, 135235.
3. Y. Y. Cai, Q. G. Zhang, A. M. Zhu and Q. L. Liu, *ACS Appl. Mater. Interfaces*, 2021, **594**, 593-603.
4. Z. Rao, M. Lan, Z. Wang, H. Wan, G. Li, J. Zhu, B. Tang and H. Liu, *J. Membrane Sci.*, 2022, **644**, 120098.
5. P. Li, J. Chen and S. Tang, *Chem. Eng. J.*, 2021, **415**, 129021.
6. Y. Li, H. Wu, Y. Yin, L. Cao, X. He, B. Shi, J. Li, M. Xu and Z. Jiang, *J. Membrane Sci.*, 2018, **568**, 1-9.
7. S. S. Liu, Z. Han, J. S. Yang, S. Z. Huang, X. Y. Dong and S. Q. Zang, *Inorg. Chem.*, 2020, **59**, 396-402.
8. S. M. Elahi, S. Chand, W. H. Deng, A. Pal and M. C. Das, *Angew. Chem. Int. Ed. Engl.*, 2018, **57**, 6662-6666.
9. Z. Shao, X. Xue, K. Gao, J. Chen, L. Zhai, T. Wen, S. Xiong, H. Hou and L. Mi, *J. Mater. Chem. A*, 2023, **11**, 3446-3453.
10. F. Yang, G. Xu, Y. Dou, B. Wang, H. Zhang, H. Wu, W. Zhou, J.-R. Li and B. Chen, *Nat. Energy*, 2017, **2**, 877-883.
11. S. Kim, B. Joarder, J. A. Hurd, J. Zhang, K. W. Dawson, B. S. Gelfand, N. E. Wong and G. K. H. Shimizu, *J. Am. Chem. Soc.,* 2018, **140**, 1077-1082.
12. Y. Yang, X. He, P. Zhang, Y. H. Andaloussi, H. Zhang, Z. Jiang, Y. Chen, S. Ma, P. Cheng and Z. Zhang, *Angew. Chem. Int. Ed. Engl.*, 2020, **59**, 3678-3684.
13. X. Y. Dong, J. H. Wang, S. S. Liu, Z. Han, Q. J. Tang, F. F. Li and S. Q. Zang, *ACS Appl. Mater. Interfaces*, 2018, **10**, 38209-38216.
14. M. Sadakiyo, T. Yamada, K. Honda, H. Matsui and H. Kitagawa, *J. Am. Chem. Soc.*, 2014, **136**, 7701-7707.
15. K. Otsubo, S. Nagayama, S. Kawaguchi, K. Sugimoto and H. Kitagawa, *JACS Au*, 2022, **2**, 109-115.
16. R.-L. Liu, W.-T. Qu, B.-H. Dou, Z.-F. Li and G. Li, *Chem-Asian J.*, 2020, **15**, 182-190.
17. S. Fan, S. Wang, X. Wang, X. Wan, Z. Fang, X. Pi, Z. Ye and X. Peng, *Sci. China Mater.*, 2021, **65**, 1076-1086.
18. S. Wang, P. Li, S. Fan, Z. Fang, X. Wang, Z. Li and X. Peng, *Dalton Trans.*, 2021, **50**, 2731-2735.
19. S.-S. Bao, N.-Z. Li, J. M. Taylor, Y. Shen, H. Kitagawa and L.-M. Zheng, *Chem. Mater.*, 2015, **27**, 8116-8125.
20. J. M. Taylor, R. K. Mah, I. L. Moudrakovski, C. I. Ratcliffe, R. Vaidhyanathan and G. K. H. Shimizu, *J. Am. Chem. Soc.*, 2010, **132**, 14055-14057.